

Inhibition of HIV-1 Rev–RRE Interaction by Diphenylfuran Derivatives<sup>†</sup>Lynda Ratmeyer,<sup>‡</sup> Maria L. Zapp,<sup>§</sup> Michael R. Green,<sup>||</sup> Ravi Vinayak,<sup>⊥</sup> Arvind Kumar,<sup>‡</sup> David W. Boykin,<sup>‡</sup> and W. David Wilson<sup>\*,‡</sup>

Department of Chemistry and Center for Biotechnology and Drug Design, Georgia State University, Atlanta, Georgia 30303, Department of Molecular Genetics and Microbiology/Cancer Center and Howard Hughes Medical Institute, University of Massachusetts Medical Center, Worcester, Massachusetts 01605, and Perkin Elmer, Applied Biosystems Division, 850 Lincoln Centre Drive, Foster City, California 94404

Received April 19, 1996; Revised Manuscript Received August 5, 1996<sup>®</sup>

**ABSTRACT:** The interactions between RNA structures, such as RRE in the HIV-1 genome, and proteins, such as Rev of HIV-1, are essential for efficient viral replication. Compounds that bind specifically to such RNAs and disrupt their protein complexes offer a novel mechanism for inhibition of replication of the virus. As a step in this approach, we have designed and characterized a series of synthetic diphenylfuran cations that selectively inhibit Rev binding to RRE. Fluorescence titrations and gel band-shift results indicate that the diphenylfurans bind to RRE and inhibit Rev complex formation in a structure-dependent manner. The derivative with the greatest affinity for RRE has an association constant of greater than  $10^7$  M<sup>-1</sup> and inhibits formation of the Rev–RRE complex at concentrations below 1  $\mu$ M. It binds to RRE considerably more strongly than it binds to simple RNA duplexes. Spectral changes and energy transfer results on complex formation suggest that the compound has a nonclassical intercalation binding mode. CD studies with modified RRE hairpins indicate that the active diphenylfurans bind at the structured internal loop of RRE and cause a conformational change. The most active diphenylfurans are tetracations that appear to bind to RRE by a threading intercalation mode and cause a conformational change in the RNA that is essential for inhibition of Rev complex formation with RRE.

RNA viruses are responsible for a number of serious human diseases, and attempts to design drugs against such viruses are proceeding along several lines (Vaishnav & Wong-Staal, 1991; Mitsuya et al., 1990; DeClerq, 1990; Haseltine, 1989). Viral genomic RNA contains sequences, such as TAR and RRE of HIV-1, that can be folded into compact conformations with sections of A-form helix containing loops, bulges, and base-pair mismatches that strongly affect the local RNA conformation (Le et al., 1988; Hauber & Cullen, 1988; Ahmed et al., 1990; Feng & Holland, 1988; Karn et al., 1991; Green, 1993; Bartel et al., 1991; Dayton et al., 1992). The folded RNA conformational units are specifically recognized by regulatory proteins (Nagai & Mattaj, 1994), are critical for viral replication (Feng & Holland, 1988; Karn et al., 1991; Selby et al., 1989; Weeks et al., 1990; Weeks & Crothers, 1991; Dingwall et al., 1990) and, thus, offer attractive potential targets for design of drugs to inhibit viral transcription.

The discovery that neomycin is a very strong and selective inhibitor of the binding of the regulatory protein Rev to RRE (Zapp et al., 1993) clearly demonstrates that drugs that target RNA can be developed as antiviral agents. In previous studies, we investigated the interaction of a number of very

different compounds with corresponding RNA and DNA duplexes in order to define a library of molecular structures and substituents that provide enhanced RNA duplex interactions, selectivity, and affinity (Wilson et al., 1993; McConnaughie et al., 1994). Our long-term goal in these studies is to define classes of compounds that bind to viral RNA structures which are highly conserved and essential for replication. Generation of additional compounds in the active classes along with studies of their RNA complexes will provide structure–activity information for development of RNA structure-specific anti-HIV-1 drugs.

We previously studied the interaction of diphenylfuran derivatives (Table 1) with DNA model systems, and we found that they can exhibit both sequence and structure dependent binding modes. In AT sequences of DNA the furans generally bind strongly in the minor groove as with well-characterized unfused aromatic cations such as netropsin (Boykin et al., 1995; Wilson et al., 1990). In other sequences of DNA, the furans bind by intercalation (e.g., compounds such as **1** and **2**) or by a weak external electrostatic interaction (e.g., compounds such as **4** and **5**) depending on the nature of the cationic substituents (Wilson et al., 1990; Zhao et al., 1995). In a recent study of the interaction of diphenylfurans with the RNA polymer duplex, polyA·polyU, we have found that they display a wide range of binding affinities and modes. Furimidazoline, **2**, binds very strongly to the RNA duplex by an intercalation mode (Zhao et al., 1995) while tetracation **8** binds strongly with the diphenylfuran system intercalated and the alkylamine substituents in a groove of the A-form RNA helix (Zhao et al., 1995).

In the studies reported here we found that specific furan derivatives bind much more strongly to RRE than to simple RNA duplex structures and that the furans effectively

<sup>†</sup> This work was supported by NIH Grants to W.D.W., D.W.B., M.R.G., and M.L.Z.

\* To whom correspondence should be addressed. Tel: (404) 651-3903. FAX: (404) 651-1416. E-mail: chewdw@gsusg1.gsu.edu.

<sup>‡</sup> Georgia State University.

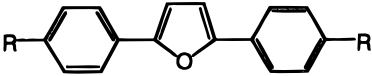
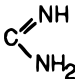
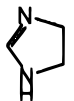
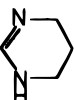
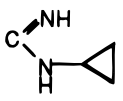
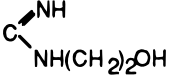
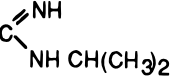
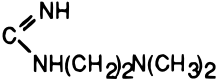
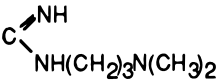
<sup>§</sup> Department of Molecular Genetics and Microbiology/Cancer Center, University of Massachusetts Medical Center.

<sup>||</sup> Howard Hughes Medical Institute, University of Massachusetts Medical Center.

<sup>⊥</sup> Perkin Elmer.

<sup>®</sup> Abstract published in *Advance ACS Abstracts*, October 1, 1996.

Table 1: Rev-RRE Complex Inhibition, Molar  $\theta$ , and Binding Constants

		IC <sub>50</sub> (mM)	RRE				polyA·polyU $\Delta T_m$
			$\theta_{350nm}$ $\times 10^{-4}$ <sup>a</sup>	$\delta\theta_{260nm}$ $\times 10^{-4}$ <sup>a</sup>	$K \times 10^{-5}$ <sup>b</sup>	$n^b$	
1	R = 	1–5	0.20	–0.25	5.0	2	6.8
2		1	0.20	–0.13	60	3	14.5
3		10	0.05	–0.11	0.8	–	2.5
4		100	0.09	–0.11	1.1	–	2.5
5		10–100	0.05	–0.12	0.5	–	4.0
6		100	0.04	–0.11	0.9	–	1.5
7		5	0.14	–0.40	200	2	9.0
8		<1	0.20	–0.40	300	2	8.5
neomycin B		1	–	+0.60			
kanamycin A		>100	–	0			

<sup>a</sup> Molar  $\theta$  values were calculated from the plots in Figure 2. <sup>b</sup>  $K$  (per RRE strand) and  $n$  values were calculated from Scatchard plots, Figure 5c. <sup>c</sup> From Zhao et al. (1995).

compete with Rev for binding to RRE. The interactions of these compounds with RRE are much more sensitive to structural variations than their interactions with simple RNA duplexes. For analysis of the furan derivative interactions with RRE, we have used an RRE hairpin model (Figure 1) similar to those studied in NMR experiments (Battiste et al., 1994, 1995; Peterson et al., 1994). This RNA sequence represents the high-affinity Rev binding site on RRE and contains two RNA duplex stems that enclose an internal loop with unusual purine·purine base pairs and two base bulges (Bartel et al., 1991; Battiste et al., 1994, 1995; Peterson et al., 1994; Iwai et al., 1992). We have conducted parallel experiments with neomycin and kanamycin, two aminoglycoside antibiotics which have similar structures but cause quite different levels of Rev-RRE inhibition (Zapp et al., 1993).

## MATERIALS AND METHODS

**Materials.** PolyA·polyU (Sigma) was characterized as previously described (Tanious et al., 1992). Neomycin, kanamycin, and ethidium bromide were purchased from Sigma. Experiments were conducted in 0.01 M piperazine-*N,N'*-bis(2-ethanesulfonic acid), 1 mM EDTA and 0.1 M NaCl buffers at pH 7.0, except for the CD experiments in which 3.75 mM NaH<sub>2</sub>PO<sub>4</sub>, 1 mM EDTA, and 0.1 M NaCl buffers at pH 7.0 were used in order to measure the oligomer CD at lower wavelengths. Syntheses of **1–3** (Boykin et al., 1995) and **7** and **8** (Zhao et al., 1995) have been published

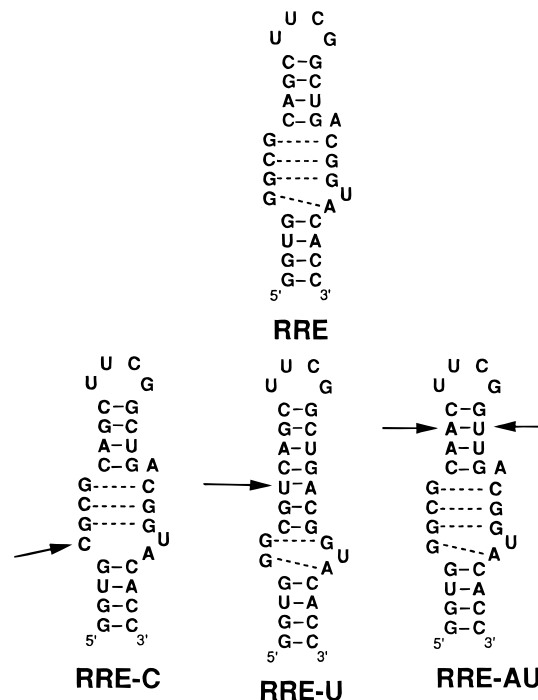


FIGURE 1: RRE hairpin models. Structures for the RRE RNA hairpin system (Bartel et al., 1991) and three mutants used in the studies described here are shown.

previously, and syntheses of **4–6** will be published elsewhere (Boykin et al., manuscript in preparation).

**RRE Syntheses.** The RNA sequences were synthesized on an Applied Biosystems 394 DNA/RNA synthesizer at 1  $\mu$ mole scale. The RNA phosphoramidites and supports (Applied Biosystems) bear phenoxyacetyl as the exocyclic amine protecting group for adenosine, *N*-(dimethylamino)-methylene for guanosine and isobutyryl for cytidine (Applied Biosystems User Bulletin, 1994). Deprotection of the base-protecting groups was complete in 4 h at 55 °C in a mixture of 3:1 ammonium hydroxide:ethanol. The *tert*-butyldimethylsilyl protecting groups were removed with a neat solution of triethylamine trihydrofluoride (10  $\mu$ L/ODU, 24 h at ambient temperature). The crude RNA was precipitated by the addition of 1-butanol (100  $\mu$ L/ODU) to the above solution. These were analyzed and purified by anion-exchange HPLC (NucleoPac PA-100, 250  $\times$  9 mm, Dionex Corporation) with a flow rate of 1.0 mL/min and a gradient of 20 mM LiClO<sub>4</sub> + 20 mM NaOAc in 9:1 H<sub>2</sub>O:CH<sub>3</sub>CN (pH 6.5) (Solvent A) to 70% of 600 mM LiClO<sub>4</sub> + 20 mM NaOAc in 9:1 H<sub>2</sub>O:CH<sub>3</sub>CN (pH 6.5) (Solvent B) in 40 min. The purified RNA was isolated by the addition of 1-propanol (3–4 vol) to the fractions with product (Sproat et al., 1995).

**Thermal Melting Studies.**  $T_m$  experiments were conducted with a Cary 4 spectrophotometer interfaced to a Dell/486 microcomputer, as previously described (Kibler-Herzog et al., 1990). Experiments were conducted in 1 mL of buffer in 1-cm path length reduced-volume quartz cells with  $1.1 \times 10^{-6}$  M RRE strand concentration or  $1.0 \times 10^{-4}$  M RNA polymer base pair, and  $T_m$  values were determined from first-derivative plots.

**Absorption and Fluorescence Spectra.** Absorption spectra for the diphenylfuran derivatives ( $3 \times 10^{-6}$  M) in the presence of a variety of either RRE or polyA·polyU concentrations were recorded from 300 to 500 nm on a Cary 4 spectrophotometer. Similar fluorescence emission spectra were recorded from 360 to 600 nm on an SLM 8000C spectrofluorimeter, with  $\lambda_{ex} = 358$  nm. The RRE experiments were performed at 5 °C, and the RNA polymer experiments were performed at room temperature. Spectra for the RNA polymer experiments were previously reported (Zhao et al., 1995).

**Binding Affinity.** Fluorescence emission spectra of the furans in 1-cm path length cells at 5 °C were obtained at increasing concentrations of RRE until no further change in fluorescence was observed. In Benesi–Hildebrand plots, the reciprocal of change in fluorescence was plotted versus the reciprocal of the RRE strand concentration, and  $I_b$  values were determined by extrapolation to  $1/[RRE] = 0$ . The concentration of bound furan derivative ( $C_b$ ) was calculated from  $C_b = [(I_o - I_i)/(I_o - I_b)]C_t$ , where  $I_o$  is the fluorescence intensity of the compound in the absence of the nucleic acid,  $I_i$  is the intensity in the presence of each concentration of nucleic acid,  $I_b$  is fluorescence intensity of the compound bound to the RNA, and  $C_t$  is the total concentration of the compound. A variety of  $C_t$  values ( $1 \times 10^{-8}$  to  $5 \times 10^{-6}$  M) of the furans were used in order to define the binding isotherms for each of the derivatives. In Scatchard plots, data were plotted as  $\nu/C_{free}$  versus  $\nu$ , where  $\nu$  is the ratio  $C_b/[RRE \text{ strand}]$  and  $C_{free}$  is the concentration of free compound. Only data in the bound fraction range 0.1–0.9 were used in Scatchard plots.

**Energy Transfer.** In energy transfer experiments, absorption spectra for the free drug, free nucleic acid, and drug–nucleic acid complex were recorded from 230 to 460 nm

and compared to corresponding excitation fluorescence spectra, with  $\lambda_{em} = 460$  nm. Experiments were conducted in 1-cm path length cells with  $2 \times 10^{-7}$  M compound and  $5.8 \times 10^{-6}$  M RRE strand or polyA·polyU base pair. The RRE experiments were at 5 °C, and the RNA polymer experiments were at room temperature.

**Circular Dichroism.** CD spectra were obtained with a Jasco J-710 spectrophotometer interfaced to a microcomputer as previously described (Zuo et al., 1990). All experiments were performed in 1-cm path length cuvettes with  $2.0 \times 10^{-6}$  M RRE strand or  $1.0 \times 10^{-4}$  polymer base concentration and with several ratios of compound to nucleic acid RRE strand, from 1 to 10, or to polymer nucleic acid base pair, from 0.1 to 0.6. RRE experiments were performed at 5 °C, and the polymer experiments were performed at room temperature. The RNA polymer CD experiments were previously reported in Zhao et al. (1995).

**Gel Mobility Shift Assay.** A 67-nucleotide RRE probe labeled with [<sup>32</sup>P]GTP was transcribed *in vitro* using T7 RNA polymerase (Promega), purified, and quantitated as previously described (Zapp & Green, 1989). Rev protein was purified from *Escherichia coli* using affinity chromatography, analyzed by immunoblotting with anti-Rev antibodies, and visualized by silver staining. Rev-RNA binding reactions were performed in 40 mM Tris-HCl (pH 7.9), 50 mM KCl, 1 mM dithiothreitol, 2 mM phenylmethylsulfonyl fluoride and typically contained 1.3 ng of purified Rev, 5 fmol of RRE RNA, 4 units of RNasin (Promega), and 19  $\mu$ g of yeast tRNA (Sigma). Rev–RRE complexes in the absence or presence of drugs were analyzed using a gel mobility shift assay and visualized by autoradiography as previously described (Zapp et al., 1993).

## RESULTS

**RRE Complexes. Thermal Melting Studies.** Relative affinities of compounds for nucleic acids can be compared by the increases they produce in the  $T_m$  of the nucleic acid upon complex formation (Crothers, 1971). The  $T_m$  values for complexes of the diphenylfuran compounds with the RNA polymer, polyA·polyU, have been reported elsewhere (Zhao et al., 1995) but are listed in Table 1 for reference. Equilibrium binding constants ( $K$ ) for interaction of the compounds with polyA·polyU were approximated from the  $\Delta T_m$  values at saturation binding (Crothers, 1971) by using the  $\Delta H^\circ$  value for polyA·polyU from Krakauer and Sturtevant (1968), a polymer RNA binding site size of three base pairs, and free ligand concentration of  $1 \times 10^{-5}$  M. The order of binding constants for the compounds with the polymer RNA is **2** > **7**, **8** > **1** > **5** > **3**, **4**, **6**, and the  $K$  values range from 0.3 to  $3 \times 10^5$  for  $\Delta T_m$  values from 2.5 to 14.5 °C, respectively.

Thermal melting curves for the RRE hairpin are somewhat broad and asymmetric but are reversible on heating and cooling at a rate of 0.5° per minute (not shown). In our standard 0.1 M NaCl buffer the melting transition is centered at 60–70 °C. Addition of the furans of Table 1 causes the curves to shift to higher temperature, but the asymmetry of the broad curves precludes  $T_m$  calculation. Compound **8** causes the largest shift in the  $T_m$  curve (over 10 °C) to higher temperature, and shifts with other furans are smaller.

**RRE Complexes. Spectral Changes.** In order to obtain more specific information on the complexes of the furan

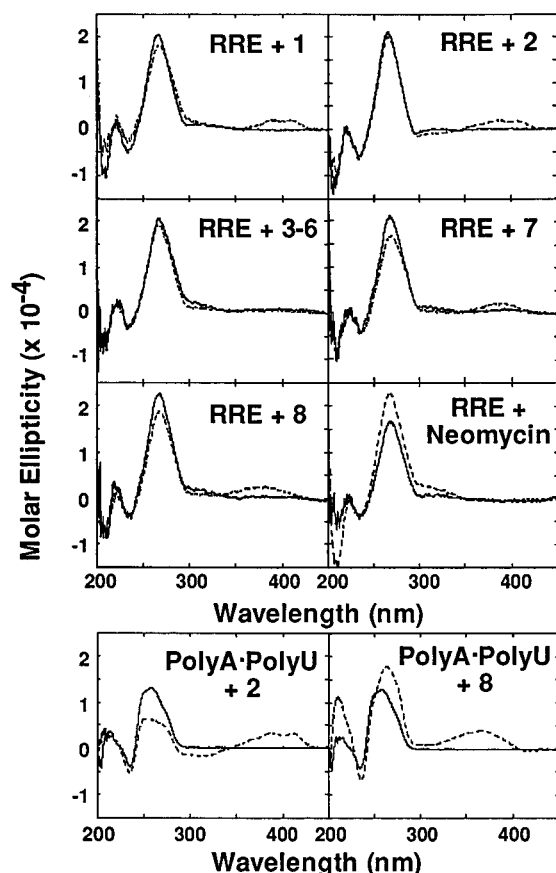


FIGURE 2: RNA complex CD spectra. CD spectra for RRE or polyA·polyU (solid lines) with the diphenylfurans or neomycin (dashed lines) at saturating ratios of compound per mole of RRE strand. Spectra for RRE with compounds 3–6 are quite similar, and only the result for 3 is shown as a representative example. Experiments were conducted with  $2.0 \times 10^{-6}$  M RNA hairpin concentration.

compounds with RRE, CD (Figures 2 and 3), UV–visible (Figure 4A) and fluorescence spectra (Figure 4B) were obtained. There are pronounced CD spectral changes on complex formation between some compounds and RRE (Figure 2). The compounds have no chiral centers and no CD spectra until they complex with the nucleic acid. For the diphenylfuran complexes with RRE, significant positive induced CD bands are seen in the 360–400 nm region in the spectra for compounds 1, 2, 7, and 8 while no significant bands are seen in the same region in the spectra for compounds 3–6. An A-form helix CD spectrum is observed below 300 nm for RRE (Figure 2), and the peak at 265 nm decreases on complex formation with the furans. The RRE CD band at 265 nm increases dramatically on complex formation with the Rev inhibitor neomycin but has no significant change when complexed with the inactive compound kanamycin. There are no long-wavelength absorption transitions for neomycin and kanamycin.

CD spectral changes for polyA·polyU with these diphenylfurans have been published recently (Zhao et al., 1995), and those for 2 and 8 are displayed in Figure 2 for comparison with those of RRE. Compound 2 binds polyA·polyU by intercalation, and the CD spectrum for this complex has a positive long wavelength induced CD band and a significant reduction in the intensity of the 265 nm RNA CD band. Compound 8 binds by intercalation with the cationic substituents in an RNA groove, and the spectrum for the complex of 8 with polyA·polyU has both an induced

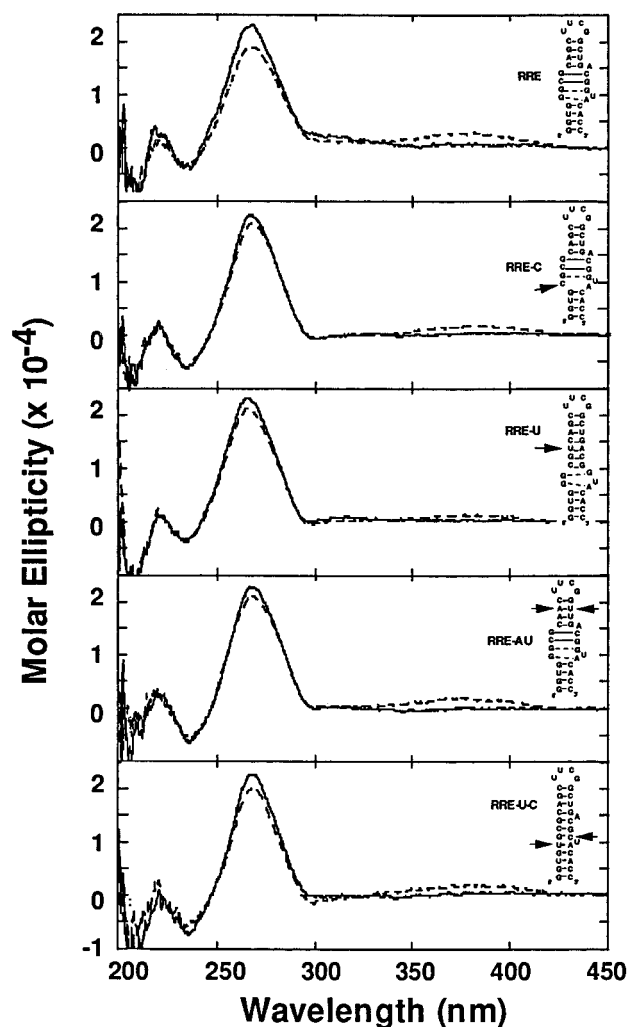


FIGURE 3: RRE and mutant CD spectra with tetracycline 8. CD spectra of RRE (solid lines) with 8 (dashed lines) compared to spectra for complexes with RRE hairpins that have base modifications (Figure 1). Changes in molar ellipticity at the furan  $\lambda_{\max}$  (360–400 nm) are as follows: RRE,  $0.25 \times 10^4$ ; RRE-C,  $0.17 \times 10^4$ ; RRE-U,  $0.13 \times 10^4$ ; RRE-AU,  $0.24 \times 10^4$ ; and RRE-U-C,  $0.18 \times 10^4$ . Changes in molar ellipticity at the RNA  $\lambda_{\max}$  ( $\sim 265$  nm) are as follows: RRE:  $0.40 \times 10^4$ ; RRE-C,  $0.09 \times 10^4$ ; RRE-U,  $0.23 \times 10^4$ ; RRE-AU,  $0.18 \times 10^4$ ; and RRE-U-C,  $0.25 \times 10^4$ . Experiments were conducted with  $2.0 \times 10^{-6}$  M RNA hairpin concentration.

positive long-wavelength CD band and a significant increase in the intensity of the 265 nm RNA band (Zhao et al., 1995).

CD experiments were also carried out on complexes of 8 with RRE model systems (Figure 1) that have modified sequences (Figure 3). CD spectra for complexes of 8 with the hairpin that has modifications in the stem region between the hairpin and internal loop regions, RRE-AU, have induced spectral changes that are similar to those induced in the spectra of the unmodified RRE. The CD spectra of the duplexes having modifications in the internal loop region, RRE-C, RRE-U, and RRE-U-C, have decreased induced long-wavelength bands. The positive CD band at 265 nm for the modified RRE hairpins decreases on complex formation with 8; however, the decrease in this CD band for the modified RRE hairpins is less than that for the unmodified hairpin complexed with 8.

UV–visible spectra of 1–8 show pronounced shifts to longer wavelengths and decreases in extinction coefficients on binding to RRE (Figure 4A). Fluorescence spectra for

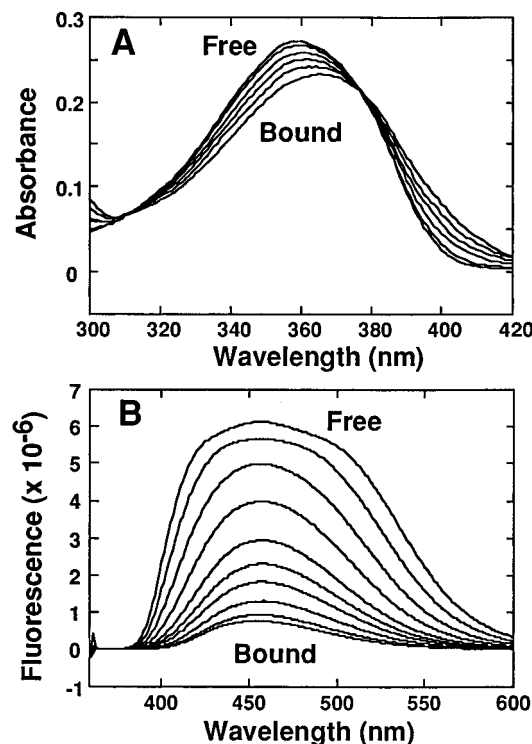


FIGURE 4: Spectral properties of RRE–8 complexes. (A) Typical UV spectral changes for the diphenylfuran complexes with RRE are illustrated with **8** ( $3 \times 10^{-6}$  M) at increasing concentrations of the hairpin RNA. (B) Fluorescence spectral changes for the diphenylfuran compounds are illustrated with the **8** ( $3 \times 10^{-6}$  M) complex with RRE at increasing concentrations of RRE hairpin.

complexes of **1–8** with RRE show intensity decreases with little shift in the maximum fluorescence wavelength (Figure 4B). Plotting change in fluorescence versus log RRE concentration (Figure 5A) shows that the compounds can be placed into two groups; **2**, **7**, and **8** require low concentrations of RRE for saturation, while **1** and **3–6** require larger concentrations of RRE for saturation.

**RNA–Compound Binding Strength.** The fluorescence decreases for furans with RRE can be followed with a high S/N ratio over a concentration range ( $10^{-8}$ – $10^{-6}$  M) that covers the region of interest for furan–RRE complexes, and the fluorescence changes provide an excellent method for determining binding constants. Comparison of all furans at a concentration of  $\sim 3 \times 10^{-6}$  M (Figure 5A) indicates that **8**, **7**, and **2** bind to RRE significantly more strongly than the other compounds from Table 1. Experiments with the strong binding compounds, **8**, **7** and **2**, were also conducted at  $\sim 2 \times 10^{-7}$  M furan concentration in order to more accurately determine the binding constants for these compounds with RRE (Figure 5A). As can be seen, **8** requires the lowest concentration of RRE for complex formation while **6** requires the highest RRE.

The fluorescence results were used to construct Benesi–Hildebrand plots (Figure 5B), as described in the Materials and Methods section. Plots for all compounds are linear and were used to determine  $I_b$  (fluorescence intensity of the bound drug), and with the fluorescence of the free compound,  $I_{free}$ , values for Scatchard plots were calculated. The Scatchard plots (Figure 5C) again confirm that there are two general groups of compounds: **8**, **7**, and **2** interact strongly with RRE, and the other compounds significantly more weakly. The Scatchard results indicate that **7** binds more strongly to

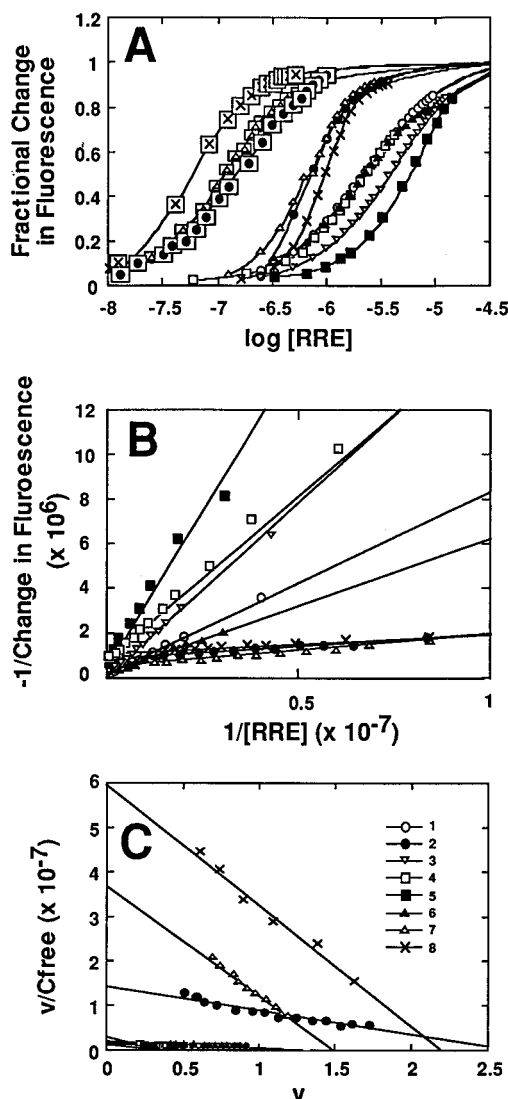


FIGURE 5: Determination of RRE–diphenylfuran affinities. (A) Changes in fluorescence for the diphenylfuran compounds on complex formation with RRE are plotted vs log(RRE hairpin concentration). Boxed symbols represent data at  $\sim 2 \times 10^{-7}$  M furan concentration, while symbols not in boxes represent data at  $\sim 3 \times 10^{-6}$  M furan. (B) Benesi–Hildebrand plots for **1–8** with RRE. (C) Scatchard plots for **1–8** with RRE. Concentrations of the compounds in B and C are  $3 \times 10^{-6}$  M (**1**, **3–6**) and  $2 \times 10^{-7}$  M (**2**, **7**, **8**).

RRE than **2** but with fewer sites, and this gives them very similar log plots in Figure 5A. Compound **8** requires the lowest concentration of RRE for binding (Figure 5A). Binding constants and number of sites on RRE are summarized for all compounds in Table 1. The exact interpretation of the binding results for these compounds depends on the  $I_b$  value and the saturation range plotted, but the experimental results in Figure 5A are unequivocal: **8**, **7**, and **2** bind to RRE very strongly and much better than the other compounds of Table 1. From the concentration of **8** required to reach 50% bound in Figure 5A, it is clear that it must have a binding constant of  $> 10^7$  M<sup>-1</sup>, and this is confirmed by the Benesi–Hildebrand and Scatchard analyses.

**RNA Binding Modes.** The CD (Figure 2), UV, and fluorescence (Figure 4) spectral shifts induced by complex formation of the furans with RRE are all characteristic of an intercalation binding mode. Energy transfer between RRE bases and **8** was evaluated from fluorescence excitation and

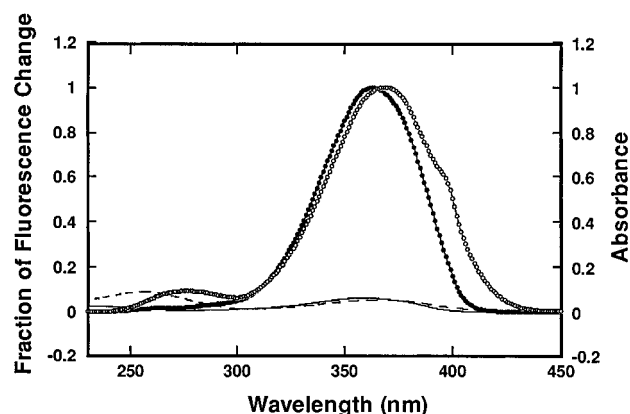


FIGURE 6: RRE-8 energy transfer. For evaluation of energy transfer from RNA bases to the diphenylfuran aromatic system, fluorescence excitation spectra for **8** ( $2 \times 10^{-7}$  M) in the absence (closed circles) and presence (open circles) of RRE ( $5.8 \times 10^{-6}$  M strand) and absorption spectra in the absence (solid lines) and presence (dashed lines) of RRE are shown. The apparent shift of the energy transfer band in the UV region to longer wavelengths than the DNA absorption peak is probably due to lamp intensity decreases in the low-wavelength UV region.

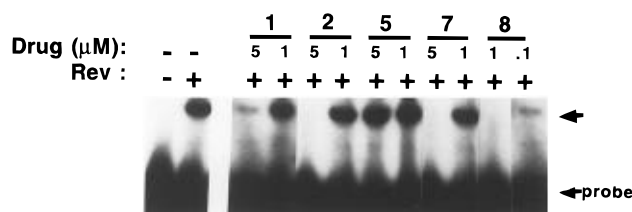


FIGURE 7: Inhibition of Rev binding to RRE by diphenylfuran derivatives. A 67-nucleotide  $^{32}\text{P}$ -labeled RNA probe containing the high-affinity Rev-binding site (nucleotides 38–104 of the RRE) was incubated with purified *E. coli*-derived Rev protein in the presence of diphenylfuran derivatives. The derivative tested and its concentration (micromolar) are indicated above each lane (Table 1). Control reactions performed in the absence of drugs are shown at the left. The absence (–) or presence (+) of Rev is indicated. The Rev–RRE complex and unbound probe are indicated by the arrowheads.

absorption spectra of the bound compound (Figure 6). A peak is observed in the excitation spectra between 260 and 290 nm, the region characteristic of base absorption, as expected for energy transfer from bases to the diphenylfuran aromatic system. In similar experiments with polyA·polyU, excitation spectra of **2** and **8**, which intercalate with polyA·polyU, have similar peaks near 260 nm (Zhao et al., 1995).

**Inhibition of Rev–RRE Complex Formation.** To evaluate the inhibition of Rev binding to RRE by the furan derivatives a labeled RRE model system was incubated with Rev protein in a gel mobility shift assay. The amount of furan required to cause dissociation of 50% of the Rev–RRE complex ( $\text{IC}_{50}$  in Table 1) was determined by conducting the gel shift assay at a range of furan derivative concentrations (Figure 7). The  $\text{IC}_{50}$  values are quite sensitive to the nature of the furan cationic group. Both dicationic and tetracationic caused inhibition of Rev binding, but the tetracation **8** is by far the best inhibitor and completely inhibits complex formation at 1  $\mu\text{M}$  concentration. It is interesting that **8** is a significantly better inhibitor than the closely related compound **7**. Formation of other RNA–protein complexes is not inhibited by **8** at the same level as the Rev–RRE complex, indicating that the inhibition is selective (not shown).

## DISCUSSION

**Diphenylfurans Bind to RRE in a Structure-Dependent Manner.** In analysis of structural effects on the binding affinity of the diphenylfuran derivatives to RNA, furamidine, **1**, serves as a useful reference. With **2** the amidine group of **1** is modified to a cyclic structure, while in **3–8** it is altered by addition of a single alkyl-based substituent to an amidine nitrogen. We have previously shown that the planar imidazoline derivative, furimidazoline, has the highest binding constant for simple RNA duplexes (Table 1) and binds to such duplexes through an intercalation mode (Zhao et al., 1995). The cationic groups in all of the other compounds (amidine derivatives) are twisted out of the diphenylfuran aromatic plane, and, as a result, they do not interact as well with intercalation sites in uniform A-type duplexes. Even though **7** and **8** are tetracations, they bind to such simple RNA duplexes more weakly than **2**, which can form a more optimally stacked intercalation complex with RNA base pairs in an A-form duplex (Table 1).

The results reported here for RRE are quite different than those with simple RNA duplexes. The diphenylfuran derivatives clearly fall into two major classes with respect to their binding affinity for RRE (Figure 5 and Table 1). The amidine tetracationic derivatives **7** and **8** along with the imidazoline dication, furimidazoline, **2**, bind much more strongly to RRE than to polyA·polyU. The other furan derivatives of Table 1 bind from ten to over a hundred times more weakly to RRE. The effects of compound structure on affinity are thus much more pronounced with RRE than with simple RNA duplexes and they follow a different structural order (Table 1). The unique conformation of RRE (Bartel et al., 1991; Battiste et al., 1994, 1995; Peterson et al., 1994) gives it an enhanced ability to discriminate among these similar organic cations that does not exist in simple RNA duplexes.

There are some parallels between the binding results of the diphenylfurans with simple RNA duplexes and the results with RRE, but it is the differences that are important. Dications **3–6** bind weakly to the simple A-form duplexes, and they also bind weakly to the RRE RNA structure. Diphenylfuran derivatives with nonplanar cyclic systems or alkyl-substituted amidine groups do not interact strongly with any of the RNAs tested to this time, and it is clear that such compounds have little potential for development as anti-Rev inhibitors. The imidazoline derivative binds more strongly to RRE than the amidine, in agreement with its stronger binding to simple RNA duplexes. It is clear, however, that **2** unlike **3–6** binds to RRE significantly more strongly than to simple RNA duplexes (Table 1). The unique structure of RRE increases the binding of **2** by over a factor of 10 relative to polyA·polyU.

Results for binding of the tetracations **7** and **8** to RRE are distinctly different than their binding to simple RNA duplexes. Both **7** and **8** bind to RRE with equilibrium constants that are approximately a factor of 100 greater than found with polyA·polyU. Simple alkyl substituents on the amidine group, for example, in **4** and **6** decrease the interactions of the diphenylfuran system with RNA, and the more polar substituent in **5** also results in a decrease in binding relative to **1**. The particularly strong binding of **7** and **8** to RRE is, thus, a result of their charged groups, but it is not a simple charge effect or they would exhibit much

stronger binding to polyA·polyU. The juxtaposition of the two charged groups on each side of **7** and **8**, along with the unique structure of the internal loop of RRE, results in a very significant enhancement of binding of these compounds to RRE relative to simple RNA duplexes. Without the charged groups, addition of substituents to the amidine, as in **3–6**, significantly weakens binding to RRE, and this makes the dramatic increase in binding on addition of the charged alkyl amines even more striking.

*Diphenylfurans Inhibit Rev Binding to RRE in a Structure-Dependent Manner.* In agreement with their binding affinities, the furans exhibit a structure-dependent inhibition of the interaction of Rev with RRE that is optimized for **8** among the compounds evaluated to this time (Figure 7, Table 1). The Rev inhibition experiments are conducted at pH 7.9, and the low activity of **7**, relative to its binding affinity (determined at pH 7), is probably due to decreased protonation of the alkylamine of **7** at the higher pH. The two methylene group separation of the amine from the strongly basic amidine group in **7** is not sufficient to insulate it from the cationic amidine charge, and the basicity of the amine is decreased in analogy to the amine groups of ethylene diamine (Perrin et al., 1981). The reduced activity of **7** at pH 7.9 strongly supports the argument that four charges are essential for optimum Rev inhibition by the diphenylfurans with substituted amidine groups. The low activity of **3–6** illustrates the high level of sensitivity of binding to the structure of the furans and is in agreement with the observed weak binding of **3–6** to all RNAs. The moderate activity of **2** is also in agreement with the relatively strong binding that this compound displays with all RNAs. Furamidine binds more weakly to RRE than furimidazoline, and it is also a weaker inhibitor of Rev binding to RRE.

The equilibrium constants for binding of the diphenylfurans to RRE are correlated with their ability to inhibit Rev binding (Table 1), and this suggests that there is a direct competition between binding of the furans and Rev to RRE. It is interesting that **8** is active at the same or even lower levels than the aminoglycoside, neomycin, which has previously been shown to be a potent inhibitor of Rev-RRE complex formation in the same assay (Zapp et al., 1993), even though the two compounds are very different in structure. The results described below indicate that there are significant differences in the mechanism of inhibition of Rev binding to RRE by neomycin and **8**.

*RRE Binding Mode of the Diphenylfurans.* In order to interpret the RRE affinities and Rev inhibition results described above, it is necessary to evaluate the binding mode of the diphenylfurans. It is now well established that the furan derivatives in Table 1 bind to DNA in the minor groove of AT sequences (Boykin et al., 1995; Wilson et al., 1990), but they can intercalate in GC sequences, where minor-groove binding is less favorable (Wilson et al., 1990). We recently reported that furan derivatives can also bind to RNA A-form duplexes by intercalation (Zhao et al., 1995), presumably due to the poor fit of the compounds into the A-form helix minor groove. The highest affinity for simple RNA duplexes is found for the imidazoline dication **2** which has an optimum fit into an RNA intercalation site, and the binding affinity for other furan derivatives is governed by their structural complementarity to the RNA intercalation site (Zhao et al., 1995).

Energy transfer is observed in the excitation spectra for **8**-RRE complexes in the spectral region characteristic of base absorption (Figure 6), and this result suggests an intercalation type of stacking interaction between the diphenylfuran ring system and bases in RRE. In support of an intercalation binding mode, the fluorescence changes induced in the furan derivatives on complex formation with RRE are characterized by a large decrease in intensity (Figure 4B). With the DNA minor-groove complexes of the furans, the fluorescence changes are quite different with only a small decrease in intensity (Wilson et al., 1990). The fluorescence changes observed for the RRE-furan complexes are similar to those observed previously on formation of intercalation complexes with GC sites in DNA (Wilson et al., 1990) and AU sites in RNA (Zhao et al., 1995) and again indicate that the furans interact strongly with the bases in RRE.

The induced CD bands in the spectra for the furan derivatives **1**, **2**, **7**, and **8** in complex with RRE are positive in the region above 350 nm where there is a strong absorption band for the furan with no interference from RNA (Figure 2 and Table 1). As shown in Figure 2, the spectra for the furan derivatives also have large induced CD bands above 350 nm when bound to polyA·polyU. The induced CD band in the spectrum with **8** is only approximately one-half as large with RRE as observed with the polyA·polyU duplex and suggests an interaction of **8** with the bases in RRE that is not a typical intercalation complex. All of the furans cause a decrease in the large positive RRE CD band near 265 nm (Figure 2 and Table 1). The tetracationic furans **7** and **8** cause the greatest decrease in this RRE CD band, while the dicationic furan **1** causes less of a decrease and **2** cause only a slight decrease in this band. These CD changes suggest that the furan-amidine derivatives **1**, **7**, and **8** cause significant conformational changes in RRE on complex formation. These results indicate that amidine derivatives are likely to be particularly effective inhibitors of Rev binding to RRE due to the conformational change that they induce on complex formation. The substituents on the amidine derivatives **3–6**, however, prevent their strong binding to RRE.

It is clear that there are quite specific structural requirements for strong binding to RRE and inhibition of Rev-RRE complex formation by the diphenylfuran derivatives. The results described above support a nonstandard intercalation model for amidine derivatives **7** and **8** that is accompanied by a significant conformational change in RRE. The smaller UV-visible and induced CD spectral changes that occur on complex formation of these derivatives with RRE relative to the changes with polyA·polyU suggest that there is less contact of the diphenylfuran ring system with bases at the intercalation site in RRE than in simple RNA duplexes. An attractive candidate for such a nonstandard intercalation complex involves a threading model in which the diphenylfuran ring system is intercalated such that the charged amidine functions are in opposite grooves. The unique structure of the RRE internal loop (Battiste et al., 1995) may facilitate formation of such a threading intercalation complex.

*RRE Binding Site for the Diphenylfurans.* The hairpin RRE model system contains a structured internal loop that can form two purine-purine base pairs with a bulged uracil base that significantly change its structure relative to A-form RNA duplexes (Bartel et al., 1991; Battiste et al., 1994, 1995;

Peterson et al., 1994). As described above, when **8** is complexed with RRE, the CD spectrum has a positive induced band above 350 nm, and the CD peak in the spectra for RRE at 265 nm decreases. With modified RNAs that have changes in the internal loop region, the spectra for **8** have significantly smaller induced CD bands above 350 nm, while, when complexed to modified RRE models with changes in one of the duplex regions, the spectra for **8** have only a slightly smaller induced CD band above 350 nm. These studies suggest that the strong binding sites for **8** on RRE are in the structured purine•purine mismatch region where two molecules of **8** can bind at saturation.

Neomycin causes an increase in the RRE CD band near 265 nm (Figure 2 and Table 1), and, as with the furan compounds, these CD changes indicate that neomycin also causes a conformational change on binding to RRE. Although the conformational changes induced in RRE by neomycin and the furans are quite different, based on the different CD results and as expected from their very different structures, in both cases the conformational changes in RRE correspond to a low IC<sub>50</sub> for inhibition of Rev binding. Kanamycin, an aminoglycoside antibiotic with a much higher IC<sub>50</sub> than neomycin (Zapp et al., 1993), causes very little change in the RRE CD band as also observed for furans **3–6** (Table 1) which are weak inhibitors of Rev–RRE complex formation.

In conclusion, synthetic diphenylfuran tetracations have been found to bind strongly to the RRE RNA of HIV-1 and inhibit complex formation with Rev. As with the aminoglycosides (Zapp et al., 1993), Rev inhibition is strongly dependent on compound structure, and the binding affinities of the furans with RRE vary much more and follow a different order than is observed with simple RNA duplexes (Table 1). The binding strength and induced CD changes for both the furans and aminoglycosides with RRE are correlated with their IC<sub>50</sub> values for Rev inhibition as determined in a gel shift assay. Neomycin, for example, is a much better inhibitor of Rev binding than the related aminoglycoside kanamycin, and neomycin induces large changes in the CD spectrum of RRE (Figure 2) while the changes induced by kanamycin are small. The changes induced in the CD spectrum of RRE by **8** are quite different from those for neomycin but are significantly larger than those for complexes of the inactive furans (Figure 2). These observations suggest that strong inhibitors of Rev binding to RRE must not only bind tightly but must also cause a significant conformational change in RRE. It is also significant that the most active diphenylfurans such as **8** do not appear to bind to RRE by classical intercalation or groove-binding modes. For example, the planar RNA intercalator **2** binds more strongly than **8** to the RNA duplex formed by polyA•polyU, but binds more weakly to RRE. CD results with modified RRE sequences indicate that the strong interaction depends on the integrity of the internal loop region of RRE, and all of our results suggest that **8** binds specifically to this unusual RNA conformation by a threading intercalation mode.

## REFERENCES

- Ahmed, Y. F., Hanly, S. M., Malim, M. H., Cullen, B. R., & Greene, W. C. (1990) *Genes Dev.* 4, 1014–1022.
- Applied Biosystems (1994) *Applied Biosystems User Bulletin*, Vol. 79.
- Bartel, D. P., Zapp, M. L., Green, M. R., & Szostak, J. W. (1991) *Cell* 67, 529–536.
- Battiste, J. L., Tan, R., Frankel, A. D., & Williamson, J. R. (1994) *Biochemistry* 33, 2741–2747.
- Battiste, J. L., Tan, R., Frankel, A. D., & Williamson, J. R. (1995) *J. Biomol. NMR* 6, 375–389.
- Boykin, D. W., Kumar, A., Spychala, J., Zhou, M., Lombardy, R. J., Wilson, W. D., Dykstra, C. C., Jones, S. K., Hall, J. E., Tidwell, R. R., Laughton, C., Nunn, C. M., & Neidle, S. (1995) *J. Med. Chem.* 38, 912–916.
- Crothers, D. M. (1971) *Biopolymers* 10, 2147–2160.
- Dayton, E. T., Konings, D., Powell, D. M., Shapiro, B. A., Butini, L., Maizel, J. U., & Dayton, A. I. (1992) *J. Virol.* 66, 1139–1151.
- DeClerq, E., Ed. (1990) *Design of Anti-AIDS Drugs*, Pharmacology Library Series, Vol. 14, Elsevier, New York.
- Dingwall, C., Erberg, I., Gait, M. J., Green, S. M., Heaphy, S., Karn, J., Lowe, A. D., Singh, M., & Skinner, M. A. (1990) *EMBO J.* 9, 4145–4153.
- Feng, S., & Holland, E. C. (1988) *Nature* 334, 165–167.
- Green, M. R. (1993) *AIDS Res. Rev.* 3, 41–55.
- Haseltine, W. A. (1989) *J. Acquired Immune Defic. Syndr.* 2, 311–334.
- Hauber, J., & Cullen, B. R. (1988) *J. Virol.* 62, 673–679.
- Iwai, S., Pritchard, C., Mann, D., Karn, J., & Gait, M. J. (1992) *Nucleic Acids Res.* 20, 6465–72.
- Karn, J., Dingwall, C., Finch, J. T., Heaphy, S., & Gait, M. J. (1991) *Biochimie* 73, 9–16.
- Kibler-Herzog, L., Kell, B., Zon, G., Shinozuka, K., Mizan, S., & Wilson, W. D. (1990) *Nucleic Acids Res.* 18, 3545–3555.
- Krakauer, H., & Sturtevant, J. M. (1968) *Biopolymers* 6, 491–512.
- Le, S.-Y., Chen, J.-H., Braun, M. J., Gonda, M. A., & Maizel, J. V. (1988) *Nucleic Acids Res.* 16, 5153–5169.
- McConnaughie, A. W., Spychala, J., Zhao, M., Boykin, D. and Wilson, W. D. (1994) *J. Med. Chem.* 37, 1063–1069.
- Mitsuya, H., Yarchoan, R., & Broder, S. (1990) *Science* 249, 1532–1544.
- Nagai, K. and Mattaj, I. W., Eds. (1994) *RNA–Protein Interactions*, Oxford-IRL Press, Oxford.
- Perrin, D. D., Dempsey, B., & Serjeant, E. P. (1981) *pK<sub>a</sub> Prediction for Organic Acids and Bases*, Chapman and Hall, London.
- Peterson, R. D., Bartel, D. P., Szostak, J. W., Horvath, S. J., & Feigon, J. (1994) *Biochemistry* 33, 5357–5366.
- Selby, M. J., Bain, E. S., Luciw, P. A., & Peterlin, B. M. (1989) *Genes Dev.* 3, 547–558.
- Sproat, B., Colonna, F., Mullah, B., Tsou, D., Andrus, A., Hampel, A., & Vinayak, R. (1995) *Nucleosides Nucleotides* 14, 255–273.
- Tanious, F. A., Veal, J. M., Buczak, H., Ratmeyer, L. S., & Wilson, W. D. (1992) *Biochemistry* 31, 3103–3112.
- Vaishnav, Y. N., & Wong-Staal, F. (1991) *Annu. Rev. Biochem.* 60, 577–630.
- Weeks, K. M., & Crothers, D. M. (1991) *Cell* 66, 577–588.
- Weeks, K. M., Ampe, C., Schultz, S., Steitz, T. A., & Crothers, D. M. (1990) *Science* 249, 1281–85.
- Wilson, W. D., Ratmeyer, L., Zhao, M., Strekowski, L., & Boykin, D. (1993) *Biochemistry* 32, 4098–4104.
- Wilson, W. D., Tanious, F. A., Buczak, H., Venkatramanan, M. K., Das, B. P., & Boykin, D. W. (1990) *Molecular Basis of Specificity in Nucleic Acid–Drug Interactions* (Pullman, B., & Jortner, J., Eds.) pp 331–353, Kluwer Academic Publishers, The Netherlands.
- Zapp, M., & Green, M. (1989) *Nature* 342, 714–716.
- Zapp, M. L., Stern, S., & Green, M. R. (1993) *Cell* 74, 969–978.
- Zhao, M., Ratmeyer, L., Peloquin, R., Yao, S., Kumar, A., Spychala, J., Boykin, D. W., & Wilson, W. D. (1995) *J. Bioorg. Med. Chem.* 3, 785–794.
- Zuo, E. T., Tanious, F. A., Wilson, W. D., Zon, G., Tan, G.-S., & Wartell, R. M. (1990) *Biochemistry* 29, 4446–4456.